Journal of Power Sources 248 (2014) 660–667

Contents lists available at ScienceDirect

Journal of Power Sources

journal homepage: www.elsevier.com/locate/jpowsour

Enhancement of photovoltaic performance of photoelectrochemical biofuel cells by β-functionalized porphyrin sensitizers

Jing Yang [a], Bin Wang [b], Yingfang Liu [a], Kunqi Wang [a], Wei Xing [a,*], Changpeng Liu [a,*]

[a] State Key Laboratory of Electroanalytical Chemistry, Changchun Institute of Applied Chemistry, Laboratory of Advanced Power Sources, Graduate School of the Chinese Academy of Sciences, 5625 Renmin Street, Changchun 130022, PR China
[b] Flight Research Institute, Aviation University of Air Force, 2222 Nanhu Road, Changchun 130022, PR China

HIGHLIGHTS

- A calculation is used to analyze series of porphyrins as sensitizers.
- Photoelectrochemical biofuel cells were fabricated with the above porphyrins.
- The haematoporphyrin showed the best performance of the series of porphyrins.
- The theoretical calculation was consistent with the experimental results.

ARTICLE INFO

Article history:
Received 14 May 2013
Received in revised form
23 July 2013
Accepted 9 August 2013
Available online 19 August 2013

Keywords:
Photovoltaic performance
Sensitizer
Porphyrin
Photoelectrochemical biofuel cell
Density functional theory

ABSTRACT

Extending excited-state of sensitizer that absorbs visible photon and produces charge separation is of importance for a photoelectrochemical biofuel cell (PEBFC). In the present work, the dependence of series of porphyrins functionalized at β-positions as sensitizers' structures on their excited-state are analyzed with the density functional theory and time-dependent density functional theory. The calculated results expect that the radiative lifetime decreases in the order of haematoporphyrin > protoporphyrin IX > H_2-mesoporphyrin IX. The designed PEBFCs with the above porphyrins as sensitizers are assembled, in which the photocurrent action spectra testifies that the order of the radiative lifetime is consistent with that of the incident photon-to-collected electron conversion efficiency (IPCE) value based on the series of porphyrins. All the experimental characteristics show that the porphyrin with ethanol group (−CHOH−CH_3) at β-positions can enhance the photovoltaic performance of the PEBFC as expected.

1. Introduction

A photoelectrochemical biofuel cell (PEBFC) that combines a dye-sensitized solar cell (DSSC) [1–4] with an enzyme-catalyzed biofuel cell (BFC) [5–9] has attracted increasing research enthusiasm since Moore and co-workers have developed the new type cell (Fig. 1) [10]. The PEBFC relies upon charge separation at a dye-sensitized semiconductor photoanode, which is in close analogy with DSSC. Following photoinduced charge separation, the sensitizer cation is reduced by β-nicotinamide adenine dinucleotide (β-NADH), ultimately generating β-nicotinamide adenine dinucleotide (β-NAD^+), the oxidized form of the mediator. β-NAD^+ can serve as an electron acceptor and obtain electrons from β-D-glucose in the electrolyte under the catalysis of the glucose dehydrogenase (GDH). For the PEBFC, β-NAD^+ is not reduced at either the cathode or the photoanode, in contrast, the oxidized species, I_3^-, is reduced at the photoanode, leading to energy-wasting recombination reactions and loss of efficiency for the DSSC, and hence, charge recombination does not occur as DSSC does. In addition, for the enzyme-catalyzed BFC the efficiency is related to the stability and the immobilization of the enzyme on the electrode while for the PEBFC the enzyme is in the electrolyte and stable. Although the PEBFC has many advantages compared to the DSSC and BFC, but photovoltaic performance of the PEBFC is poor [10–19]. Amao et al. used chlorophyll or its derivative zinc chlorin-e_6 as sensitizers to construct the PEBFC which showed that short-circuit current (I_{sc}) and the open-circuit potential (V_{oc}) were 9.0 μA cm^{-2} and 415 mV, respectively. And the peaks in the photocurrent action spectrum were observed at 400 and 800 nm and the incident photon-to-collected electron conversion efficiency (IPCE) values at 400 and

* Corresponding authors. Tel.: +86 431 85262223; fax: +86 431 85685653.
E-mail addresses: xingwei@ciac.jl.cn (W. Xing), liuchp@ciac.jl.cn (C. Liu).

0378-7753/$ – see front matter © 2013 Published by Elsevier B.V.
http://dx.doi.org/10.1016/j.jpowsour.2013.08.030

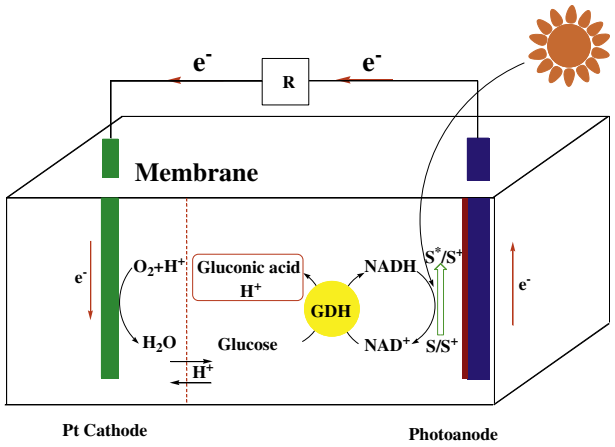

Fig. 1. Schematic diagram of the oxidation-reduction for the photoelectrochemical biofuel cell.

800 nm were estimated to be ca. 17.3% and 10.6% [16,17]. Gust et al. reported the PEBFC with 5-(4-carboxyphenyl)-10, 15, 20-*tris*(4-methylphenyl)porphyrin as a sensitizer. The PEBFC with porphyrin exhibited more performance than that with chlorophyll. The I_{sc} and V_{oc} were 55 μA cm^{-2} and 1.10 V, respectively for the PEBFC with porphyrin.

Typical sensitizer of the PEBFC is porphyrin compounds because they possess an intense Soret band at 400–450 nm and moderate Q-bands at 500–650 nm. The energy levels of the highest occupied molecular orbital (HOMO) and lowest unoccupied molecular orbital (LUMO) of porphyrin match well with the conduction band of TiO_2 molecule. We have reported the PEBFCs based on H_2-mesoporphyrin IX which exhibited the I_{sc} of 395 μA cm^{-2}, the open-circuit potential (V_{oc}) of 767 mV and meso-tetrakis (4-carboxyphenyl) porphyrin (TCPP) which exhibited I_{sc} of 69 μA cm^{-2}, V_{oc} of 740 mV [19]. The above result that the difference of the sensitizer leads to the difference of the I_{sc} and V_{oc} shows that the structure of the sensitizer has an important influence on the performance of the PEBFC. In addition, Gust et al. employed TiO_2 rather than SnO_2 as the wide band gap semiconductor of the PEBFC, which represent a significant increase in cell performance [10,11]. When the PEBFC operates with the platinum cathode under anaerobic conditions, hydrogen produces under the catalysis of the Clostridium acetobutylicum [FeFe]-hydrogenase HydA [14].

The study on the PEBFC is extensively reported [10–19], however there is no report on sensitizer structure – cell function relationship. Long excited-state of sensitizer plays an important role of injecting electrons into the conduction band of titania (TiO_2) for the PEBFC. It is obvious that the structure of sensitizer is of importance for its excited-state. In this paper, series of porphyrin compounds as sensitizers (H_2-mesoporphyrin IX, protoporphyrin IX and haematoporphyrin as shown in Fig. 2) were analyzed using the density functional theory (DFT) and time-dependent density functional theory (TD-DFT) [20–22]. With the aid of DFT and TD-DFT calculations, the HOMO, the LUMO, the energy difference between the HOMO and LUMO (ΔE_{H-L}), radiative lifetime (τ) were obtained, and the radiative lifetime decreased in the order of haematoporphyrin > protoporphyrin IX > H_2-mesoporphyrin IX [23]. The longer radiative lifetime is advantageous to injecting the electron into the conduction band of TiO_2, which is expected to enhance the photovoltaic performance of the PEBFC [23]. The experimental results showed that compared with the reported PEBFC based on H_2-mesoporphyrin IX, the PEBFCs sensitized by protoporphyrin IX or haematoporphyrin sensitizers showed much higher IPCE and better photovoltaic performance. The short-circuit current (I_{sc}) and the open-circuit potential (V_{oc}) values of the PEBFCs based on the series of sensitizers decreased in the order of haematoporphyrin > protoporphyrin IX > H_2-mesoporphyrin IX as expected. Thus, the function at β-position of the porphyrin is an important factor that must be considered for the development of the efficient PEBFC.

2. Experimental

2.1. Materials

H_2-mesoporphyrin IX, protoporphyrin IX and haematoporphyrin were purchased from J&K CHEMICAL LTD. β-NADH was purchased from Sigma–Aldrich Company. Perfluorinated sulfonic acid proton-exchange membrane Nafion 117 (thickness: 80 μm, exchange capacity: 1.0 ± 0.02 mM g^{-1}) was purchased from Shandong Dongyue Shenzhou New Material Co, Shandong China. The trishydroxylaminomethane (Tris) was obtained from J&K Chemical Ltd. GDH was obtained from Toyobo Co., Ltd. The enzyme activity was assayed following a protocol provided by the manufacturer. β-D-glucose, *N*, *N*-dimethyl formamide (DMF) and potassium chloride (KCl) were obtained from Beijing Chemical Company (Beijing, China). 3α, 7α-dihyroxy-5β-cholic acid (cheno) was obtained from Fluka. One unit of GDH activity is defined as the amount of enzyme consumed per minute that reduced 1.0 mmol NAD^+ to NADH by glucose.

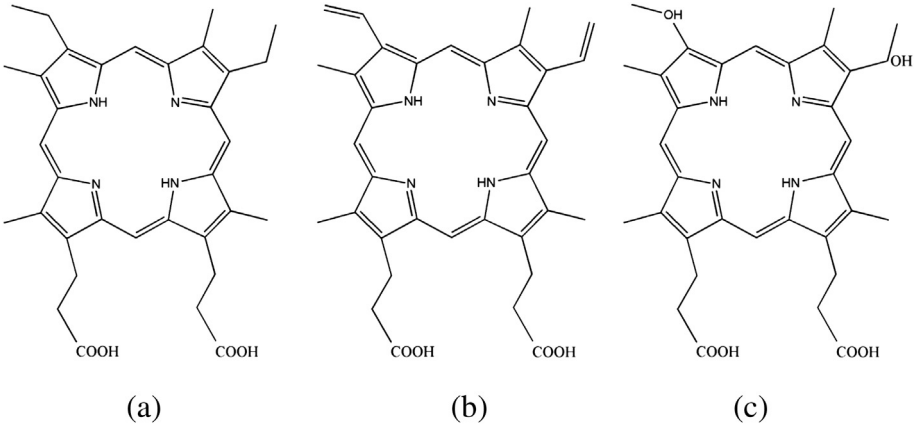

Fig. 2. Molecular structures of (a) H_2-mesoporphyrin IX, (b) Protoporphyrin IX and (c) Haematoporphyrin sensitizers.

2.2. Preparation of TiO_2 film electrode

The TiO_2 film electrode was obtained from Peng Wang group in Changchun Institute of Applied Chemistry [24].

2.3. Preparation of platinum-coated fluorine-doped tin oxide electrode

The platinum-coated FTO electrode was prepared according to the literature [19].

2.4. Fabrications of photoelectrochemical biofuel cell

The TiO_2 film electrode was heated for about 30 min at 550 °C, and then cooled to 80 °C. The above TiO_2 film electrode was dipped for 5 h in DMF solution containing 1×10^{-3} M of protoporphyrin IX or haematoporphyrin. The apparent surface area of the prepared photoanode FTO/TiO_2/protoporphyrin (or haematoporphyrin) was 0.228 cm^2.

The detailed fabrication procedures of the photoanode FTO/TiO_2/H_2-mesoporphyrin IX and the PEBFC have been reported in the previous literature [19]. The photoanode compartment was filled with 4 mM NADH, 0.1 M glucose, 0.015 units mL^{-1} GDH and 0.25 M Tris buffer solution of pH 8.0 (adjusted with HCl) that contained 0.1 M KCl as a supporting electrolyte. To remove oxygen, the photoanode compartment was saturated by nitrogen gas. The cathode compartment was filled with 0.1 M KCl and 0.25 M Tris buffer solution of pH 8.0 with saturated oxygen.

2.5. UV–Vis, Fourier transform infrared, X-ray photoelectron spectroscopy and FE-SEM measurements

The UV–Vis absorption spectra were performed on a UNICO WFZ UV-2802PC/PCS spectrometer. The Fourier Transform Infrared (FTIR) spectra were performed using a BRUKER Vertex 70 FTIR spectrometer. The TiO_2 film electrodes sensitized by protoporphyrin or haematoporphyrin were rinsed with DMF, and then dried at room temperature to measure the spectra. X-ray photoelectron spectroscopy (XPS) measurements of the TiO_2 film and FTO/TiO_2/protoporphyrin (or haematoporphyrin) electrodes were recorded by using a Kratos XSAM-800 spectrometer with Mg Kα radiator. The field-emission scanning electron microscope (FE-SEM) was carried out on the field emission microscope (JEOL, 7500B) operated at an acceleration voltage of 10 kV.

2.6. Photovoltaic characteristics

The current–voltage characteristic curve and the IPCE-wavelength measurement of the PEBFC were obtained by Labview 8.0 test bench according to the literature [19]. Electrochemical impedance spectroscopy (EIS) was obtained in a frequency range from 100 mHz to 100 kHz using EG & G PARC 18 potentiostat/galvanostat (Model 273A Princeton Applied Research Co., USA) under natural light. The amplitude of the sinusoidal potential signal was 10 mV.

2.7. Computation

All theoretical computations about the H_2-mesoporphyrin IX, protoporphyrin IX and haematoporphyrin sensitizers in this paper were carried out with DFT and TD=DFT, implementing the Gaussian 09 program package. Hybrid GGA functional, Becke's three-parameter (B3) hybrid exchange functional, incorporating the correlation functionals of Lee, Yang and Parr (LYP), namely B3LYP, was used to optimize the ground-state geometries of the three sensitizers molecules with 6-31G(d) basis set. On the basis of the ground-state geometries, HOMO, LUMO energies and HOMO-LUMO gap (ΔE_{H-L}) are obtained. TD-DFT//B3LYP/6-31G(d) is employed to optimize the lowest singlet excited-state structure, and on above basis, the radiative lifetime (τ) of H_2-mesoporphyrin IX, protoporphyrin and haematoporphyrin is obtained.

3. Results and discussion

3.1. Characterization of the photoanode

3.1.1. UV–Vis absorption spectra of dye-sensitized TiO_2 film electrode

Compared with the H_2-mesoporphyrin IX sensitizer with two ethyl groups (–CH_2–CH_3) connecting to the ring of pyrrole at β-positions (Fig. 2a), two ethyl groups (–CH_2–CH_3) are replaced by two vinyl groups (-CH = CH_2) for protoporphyrin IX (Fig. 2b) and by two ethanol groups (–CHOH–CH_3) for haematoporphyrin (Fig. 2c). In the PEBFC, the LUMO energy of the sensitizer must be suited to the conduction band edge of TiO_2, so the protoporphyrin IX and haematoporphyrin sensitizers with the reported H_2-mesoporphyrin IX were calculated to obtain their electronic states with the DFT method. The energies of HOMO, LUMO and ΔE_{H-L} for the three sensitizers are listed in Table 1. As shown in Table 1, the LUMO energies of the three sensitizers are more positive than the conduction band edge (−4.00 eV vs. vacuum) of TiO_2 [25], providing sufficient thermodynamic driving force for electron injection from the excited sensitizer to TiO_2. The calculating result shows that protoporphyrin IX exhibits a narrower ΔE_{H-L} compared to H_2-mesoporphyrin IX and haematoporphyrin, and the narrower ΔE_{H-L} is, the lower the energy needed by electronic transition from HOMO to LUMO should be, thus for protoporphyrin IX, the UV–Vis absorption spectra correspond to longer Soret band and Q-bands wavelength of absorption peak. The UV–Vis absorption spectra of protoporphyrin IX or haematoporphyrin sensitizers in a solution and at a mesoporous TiO_2 film electrode were measured so as to have a preliminary evaluation on their light-harvesting capacity as shown in Fig. 3. The two sensitizers and the reported H_2-mesoporphyrin IX in a solution all have strong light absorption in the 400–450 nm region (Soret band) and the 500–700 nm region (Q-bands) as shown in Fig. 3 and Table 2, which is in agreement with that of the respective sensitizer adsorbed at the mesoporous TiO_2 film electrode, indicating that the three sensitizers are successfully adsorbed at a mesoporous TiO_2 film electrode. Compared with H_2-mesoporphyrin IX (Fig. 3a), protoporphyrin IX (Fig. 3b) and haematoporphyrin (Fig. 3c) have longer Soret band and Q-bands wavelength of absorption peak as expected, which is shown in Table 2. The above result obviously showed that the ΔE_{H-L} of the sensitizer was closely related to the Soret band and Q-bands wavelength of UV–Vis absorption peak and the theoretical calculation could expect experimental result. The sensitizer H_2-mesoporphyrin IX coated on the mesoporous TiO_2 film electrode in the Soret band was at 407 nm, which was slightly blue-shifted by 8 nm compared with that in the solution; the absorption peaks in the Q-band region were at 507, 533, 574 and 625 nm, which were slightly

Table 1
The energies of occupied (HOMO) and unoccupied (LUMO) frontier orbitals and energy gaps for H_2-mesoporphyrin IX, protoporphyrin IX and haematoporphyrin (in eV).

Sensitizer	HOMO	LUMO	ΔE_{H-L}
H_2-mesoporphyrin IX	−5.00	−2.09	2.91
Protoporphyrin IX	−5.08	−2.22	2.86
Haematoporphyrin	−5.02	−2.11	2.91

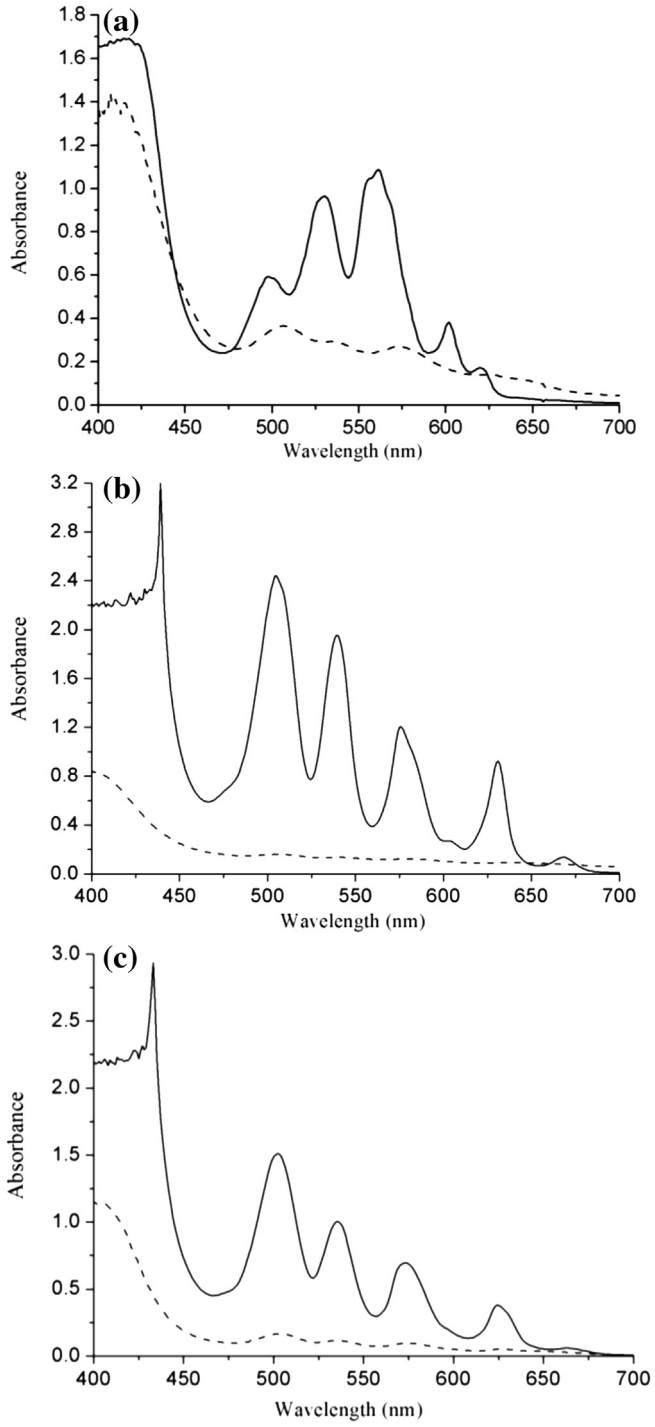

Fig. 3. (a) Absorption spectra of 5×10^{-5} M H_2-mesoporphyrin IX in ethanol solution containing 5×10^{-4} M 3α, 7α-dihyroxy-5β-cholic acid (solid line) and H_2-mesoporphyrin IX coated at TiO_2 electrode (dashed line). Absorption spectra of 1×10^{-3} M (b) protoporphyrin IX and (c) haematoporphyrin in DMF solution (solid line) and the corresponding sensitizer coated at TiO_2 electrode (dashed line).

red-shifted by 9, 3, 13 and 23 nm, compared with those in the solution, respectively (Fig. 3a). When protoporphyrin IX (Fig. 3b) or haematoporphyrin (Fig. 3c) was adsorbed at the TiO_2 film, the Soret band and Q-bands showed different shifts compared with the absorption peak of the corresponding sensitizer in the solution. The electronic coupling interaction between the π orbital of the sensitizer and the d orbital of TiO_2 resulted in the shift of the Soret band and Q-bands of the sensitizer coated on the mesoporous TiO_2 film

Table 2
The absorption peaks of UV–Vis absorption spectra for H_2-mesoporphyrin IX, protoporphyrin IX and haematoporphyrin sensitizers in a solution.

Sensitizer solution	Soret band (nm)	Q-band (nm)			
H_2-mesoporphyrin IX	415	498	530	561	602
Protoporphyrin IX	439	504	539	575	630
Haematoporphyrin	433	502	535	573	624

electrode. Therefore, the interaction between the sensitizer and the TiO_2 electrode depended on the structure of the sensitizer.

Plots of the HOMO and LUMO for the three sensitizers are shown in Fig. 4. The HOMO and LUMO for H_2-mesoporphyrin IX and haematoporphyrin are found to be mostly located on the porphyrin macrocycle, while those for protoporphyrin IX are on the porphyrin macrocycle and the two vinyl groups (−CH=CH_2). Introduction of the vinyl group for protoporphyrin IX expands the π conjugation in the sensitizer, and thus results in a wide absorption in the visible region. The absorption peaks in the Soret band and the Q-band region for porphyrin compounds are mainly attributed to the $\pi \rightarrow \pi^*$ transition from HOMO to LUMO [26–30]. The narrow ΔE_{H-L} (Table 1) explains that the absorption peaks for protoporphyrin IX in the Soret band and the Q-band region are red-shifted compared with H_2-mesoporphyrin IX and haematoporphyrin as shown in Fig. 3 and Table 2.

3.1.2. Feature of FTIR spectra

To investigate the coordination state of the protoporphyrin IX and haematoporphyrin sensitizers at the TiO_2 film, the FTIR spectra of the two sensitizers in the solid state and at the TiO_2 film were measured. Fig. 5 shows the FTIR spectra of sensitizers over the range of 500–4000 cm^{-1} at room temperature. Fig. 5A displays the FTIR spectra of TiO_2 film, the pure protoporphyrin IX powder and the protoporphyrin IX adsorbed at the TiO_2 film. The peak of C=O bond in carboxyl group was observed at 1705 cm^{-1} for the protoporphyrin IX powder. The FTIR spectrum of the protoporphyrin IX adsorbed at the TiO_2 film clearly shows the peaks at 1652 and 1459 cm^{-1}; they correspond to the asymmetric and symmetric stretching vibration of the carboxyl group, respectively, indicating that the carboxyl group is deprotonated and takes part in the adsorption of the sensitizer at the TiO_2 film [31,32]. FTIR spectrum

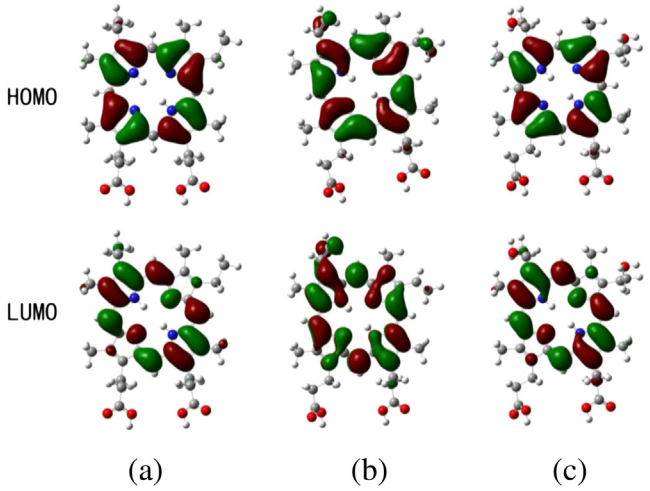

Fig. 4. Plots of the Frontier Orbitals for (a) the H_2-mesoporphyrin IX, (b) protoporphyrin IX and (c) haematoporphyrin molecules by MPW1B95/6-31G(d). (Red ball: oxygen, gray ball: carbon, white ball: hydrogen, blue ball: nitrogen.) (For interpretation of the references to colour in this figure legend, the reader is referred to the web version of this article.)

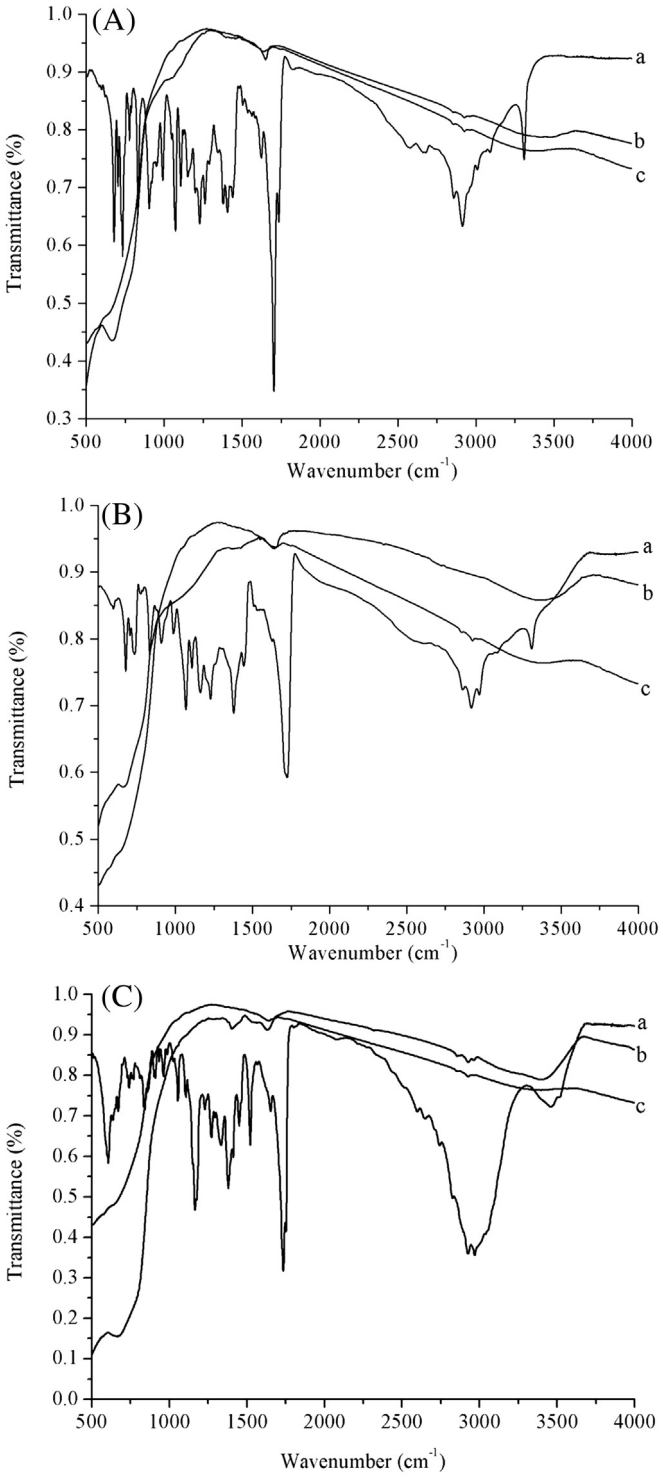

Fig. 5. (A) FTIR spectra of (a) protoporphyrin IX sensitizer, (b) the sensitizer adsorbed at a TiO_2 film and (c) TiO_2 film. (B) FTIR spectra of (a) haematoporphyrin sensitizer, (b) the sensitizer adsorbed at a TiO_2 film and (c) TiO_2 film. (C) FTIR spectra of (a) H_2-mesoporphyrin IX sensitizer, (b) the sensitizer adsorbed at a TiO_2 film and (c) TiO_2 film.

of the pure haematoporphyrin powder shows the intense peak at 1720 cm^{-1} as shown in Fig. 5B. When the haematoporphyrin was adsorbed at the TiO_2 film, two intensive peaks were observed at 1660 and 1420 cm^{-1}; the two peaks can be assigned to the asymmetric and symmetric stretching vibration of the carboxyl group, respectively. From the above FTIR data, it can be inferred that both protoporphyrin IX and haematoporphyrin are adsorbed at the TiO_2 film through the carboxyl groups via a bidentate or a bridging chelation with TiO_2 film [33], which is consistent with the observed result of the reported H_2-mesoporphyrin IX sensitizer as shown in Fig. 5C. As shown in Fig. 5, there was no obvious peak in the 500–4000 cm^{-1} range for the TiO_2 film.

3.1.3. Characterization of XPS spectra

It is known that XPS is highly correlative to surface state, so XPS is used to distinguish the surface change of pure TiO_2 before and after adsorption of protoporphyrin IX or haematoporphyrin [34–37]. Under the same conditions, the XPS of Ti (2p) and O (1s) for the TiO_2 film without any adsorption, the TiO_2 film adsorbed by protoporphyrin IX (protoporphyrin IX/TiO_2), the TiO_2 film adsorbed by haematoporphyrin (haematoporphyrin/TiO_2) and the reported TiO_2 film adsorbed by H_2-mesoporphyrin IX (H_2-mesoporphyrin IX/TiO_2) have been compared in Fig. 6. Parameters of the XPS obtained from Fig. 6 for Ti ($2p_{3/2}$), Ti ($2p_{1/2}$) and O (1s) are listed in Table 3. Compared with the peaks of the TiO_2 film without any adsorption, for the reported H_2-mesoporphyrin IX/TiO_2, the peaks of Ti ($2p_{3/2}$) and Ti ($2p_{1/2}$) showed slight red-shifts by 0.08 eV and 0.36 eV, respectively, while the red-shifts for the protoporphyrin IX/TiO_2 were 0.15 and 0.53 eV, respectively, and the red-shifts for the haematoporphyrin/TiO_2 were 0.28 and 0.70 eV, respectively (Fig. 6a). For the protoporphyrin IX/TiO_2 and haematoporphyrin/TiO_2, the red-shifts of the peaks were larger than those for the H_2-mesoporphyrin IX/TiO_2 due to the stronger interaction between the sensitizer and TiO_2. In the O (1s),

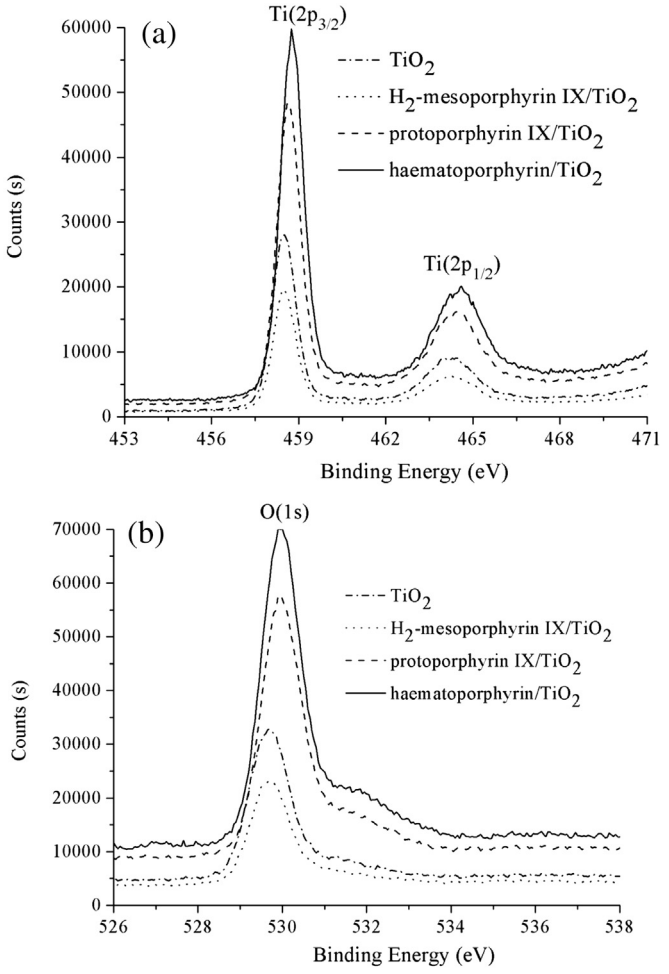

Fig. 6. XPS spectra of (a) Ti ($2p_{3/2}$), Ti ($2p_{1/2}$) and (b) O (1s) for TiO_2, H_2-mesoporphyrin IX/TiO_2, protoporphyrin IX/TiO_2 and haematoporphyrin/TiO_2.

Table 3
XPS of Ti ($2p_{3/2}$), Ti ($2p_{1/2}$) and O (1s) obtained from the curve fits of Fig. 5.

	Binding energy (eV)		
	Ti ($2p_{3/2}$)	Ti ($2p_{1/2}$)	O (1s)
TiO_2	458.47	463.91	529.68
H_2-mesoporphyrin IX/TiO_2	458.55	464.27	529.79
Protoporphyrin IX/TiO_2	458.62	464.44	529.95
Haematoporphyrin/TiO_2	458.75	464.61	530.02

similar phenomena were also observed as shown in Fig. 6b and Table 3. So the interaction between the sensitizer and TiO_2 decreased in the order of haematoporphyrin > protoporphyrin IX > H_2-mesoporphyrin IX. The strong interaction between the sensitizer and TiO_2 is in favor of electron transfer from the sensitizer to the conduction band of TiO_2 [38].

3.1.4. Characterization of FE-SEM

The SEM images of the bare TiO_2 film electrode, H_2-mesoporphyrin IX/TiO_2, protoporphyrin IX/TiO_2 and haematoporphyrin/TiO_2 were shown in Fig. 7. It was clear that the corresponding sensitizer was adsorbed on the TiO_2 surface due to the uneven surface compared with the even surface of the TiO_2 film electrode. However, H_2-mesoporphyrin IX/TiO_2, protoporphyrin IX/TiO_2 and haematoporphyrin/TiO_2 did not have obvious differences.

3.2. Photocurrent action spectrum

The PEBFC depends on charge separation at a dye-sensitized TiO_2 semiconductor film anode. The sensitizer is excited by visible photon, resulting in electron injection from the excited sensitizer into the conduction band of TiO_2. The longer the excited-state of sensitizer molecule lives, the more easily the electron is injected to the conduction band of TiO_2 [39]. The radiative lifetimes of the H_2-mesoporphyrin IX, protoporphyrin IX and haematoporphyrin sensitizers were calculated by TD-DFT//B3LYP/6-31G(d), and they were 1831.04 ns, 1838.57 ns and 1904.11 ns, respectively. And the radiative lifetime decreases in the order of haematoporphyrin > protoporphyrin IX > H_2-mesoporphyrin IX; therefore, the haematoporphyrin sensitizer with the higher radiative lifetime could have higher IPCE of the PEBFC. Moreover, the calculated energies of frontier orbitals indicate that haematoporphyrin and protoporphyrin IX have lower LUMO energy than H_2-mesoporphyrin IX as shown in Table 1, and the lower LUMO energy may endow an efficient electronic coupling of excited sensitizer with TiO_2.

The photocurrent action spectra for PEBFCs with the TiO_2 films sensitized by protoporphyrin IX, haematoporphyrin and the reported H_2-mesoporphyrin IX were shown in Fig. 8. The onset wavelengths of the IPCE spectra for the PEBFCs based on the three sensitizers were less than 750 nm. The absorption peaks in the photocurrent action spectra for the PEBFC with haematoporphyrin sensitizer were observed at 500, 560 and 656 nm, and the corresponding IPCE values were ca. 25%, 22% and 13%, respectively (Fig. 8a). For the PEBFC with protoporphyrin IX sensitizer, the corresponding IPCE values at 500, 560 and 650 nm were 22%, 20% and 11%, respectively, as shown in Fig. 8b. The IPCE values of the PEBFCs based on protoporphyrin IX or haematoporphyrin are higher than those of the reported PEBFC based on H_2-mesoporphyrin IX sensitizer (Fig. 8c). The IPCE values of the PEBFC decreased in the order of haematoporphyrin > protoporphyrin IX > H_2-mesoporphyrin IX as expected, which was consistent with the observed results from the XPS spectra and radiative lifetime. Thus, the structures of porphyrins with ethanol group (−CHOH−CH_3) or vinyl group (−CH═CH_2) at β-position are advantageous for effective electron injection from the sensitizer into the conduction band of TiO_2.

3.3. Current–voltage curve

The photoanodes with apparent surface area of 0.228 cm^2 were illuminated with 100 mW cm^{-2}; the current–voltage curves obtained for the PEBFCs with the protoporphyrin IX, haematoporphyrin and the reported H_2-mesoporphyrin IX sensitizers were shown in Fig. 9. For the three PEBFCs the current keeps constant at

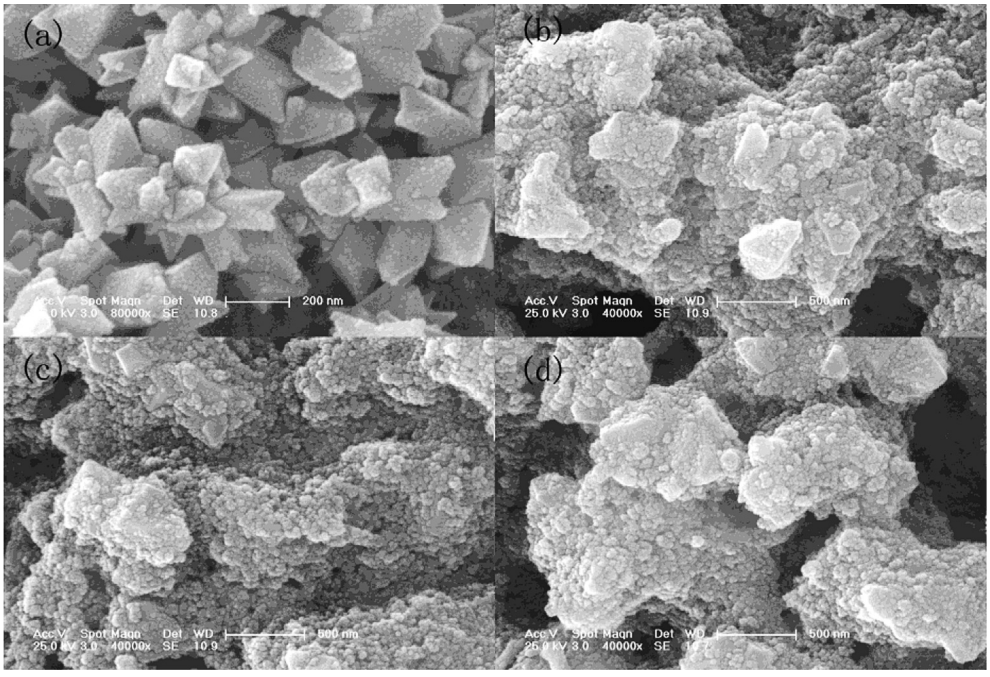

Fig. 7. The SEM images of the bare TiO_2 film electrode (a), H_2-mesoporphyrin IX/TiO_2 (b), protoporphyrin IX/TiO_2 (c) and haematoporphyrin/TiO_2 (d).

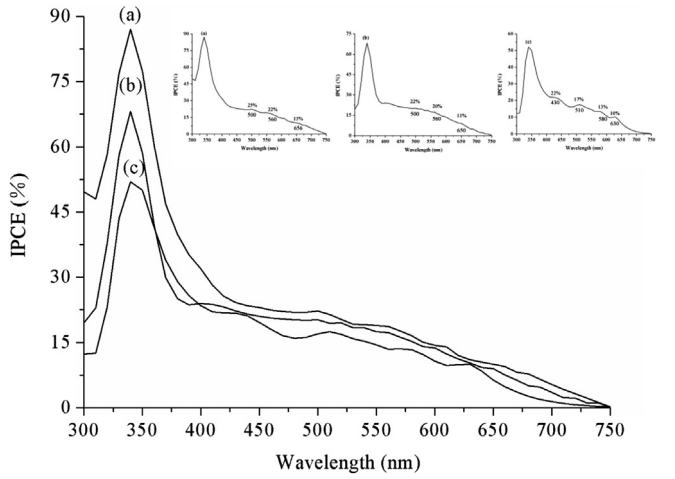

Fig. 8. Photocurrent action spectra of the photoelectrochemical biofuel cells with (a) haematoporphyrin, (b) protoporphyrin IX or (c) H_2-mesoporphyrin IX as the sensitizers.

low voltage, and then decreases with increasing voltage. However, for the PEBFC with H_2-mesoporphyrin IX, the current decreases more slowly compared to the PEBFCs with protoporphyrin IX or haematoporphyrin.

The performance characteristics of the PEBFCs were summarized in Table 4. As shown in Fig. 9 and Table 4, the short-circuit current (I_{sc}), the open-circuit voltage (V_{oc}), maximum power density (P_{max}) and fill factor (FF) of the PEBFC made from protoporphyrin IX were 94 μA, 838 mV, 134 μW cm^{-2} and 0.39, respectively (Fig. 9b). In contrast, the photovoltaic parameters, I_{sc}, V_{oc} P_{max} and FF, of the PEBFC with haematoporphyrin as a sensitizer were 100 μA, 858 mV, 118 μW cm^{-2} and 0.31, respectively (Fig. 9a). The above results show that the performance of the PEBFC is correlative with the kind of the sensitizer. Especially, the short-circuit current (I_{sc}) and the open-circuit voltage (V_{oc}) for the PEBFC with the protoporphyrin IX or haematoporphyrin sensitizer were greater than those of the PEBFC with the reprted H_2-mesoporphyrin IX sensitizer (Fig. 9c). In other words, the I_{sc} and V_{oc} values decreased in the order of haematoporphyrin > protoporphyrin IX > H_2-

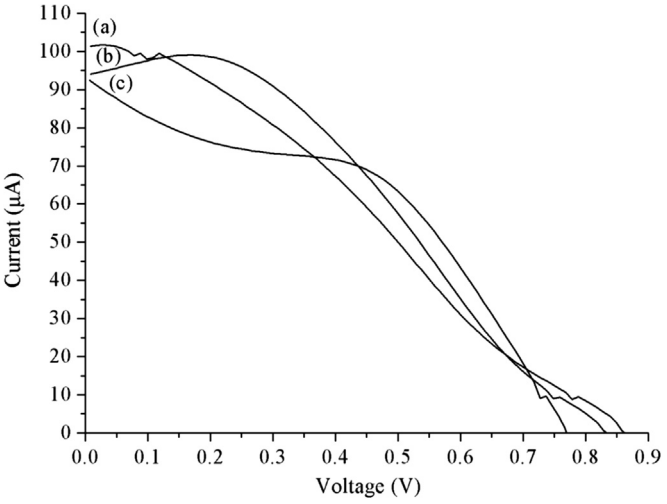

Fig. 9. Current–voltage characteristics for the PEBFCs with (a) haematoporphyrin, (b) protoporphyrin IX or (c) H_2-mesoporphyrin IX as the sensitizers under the light intensity of 100 mW cm^{-2} condition.

Table 4
Performances of the PEBFCs with H_2-mesoporphyrin IX, protoporphyrin IX or haematoporphyrin as the sensitizers.

Sensitizer	V_{oc} (mV)	I_{sc} (μA)	FF	P_{max} (μW cm^{-2})
H_2-mesoporphyrin IX	767	90	0.46	139
Protoporphyrin IX	838	94	0.39	134
Haematoporphyrin	858	100	0.31	118

mesoporphyrin IX. However, the corresponding FF values were lower than that of the reported PEBFC with the H_2-mesoporphyrin IX sensitizer. The FF is defined as the ratio of the maximum power P_{max} obtained with the device and the theoretical maximum power, that is FF = $P_{max}/I_{sc}V_{oc}$. The FF can then take values between 0 and 1. It reflects electrical and electrochemical losses occurring during operation of the PEBFC. The FF value increased in the order of haematoporphyrin < protoporphyrin IX < H_2-mesoporphyrin IX, which stemmed from the higher I_{sc} and V_{oc} for the PEBFCs with protoporphyrin IX or haematoporphyrin sensitizers and showed that the sensitizer influenced losses during operation of the PEBFC.

Next let us focus on the long-time performance of the three PEBFCs against continuous irradiation. After 24 h irradiation with the light intensity of 100 mW cm^{-2} xenon lamp, only little current and voltage changes are observed (±4.5%), indicating that the three PEBFCs are stable against irradiation within 24 h irradiation.

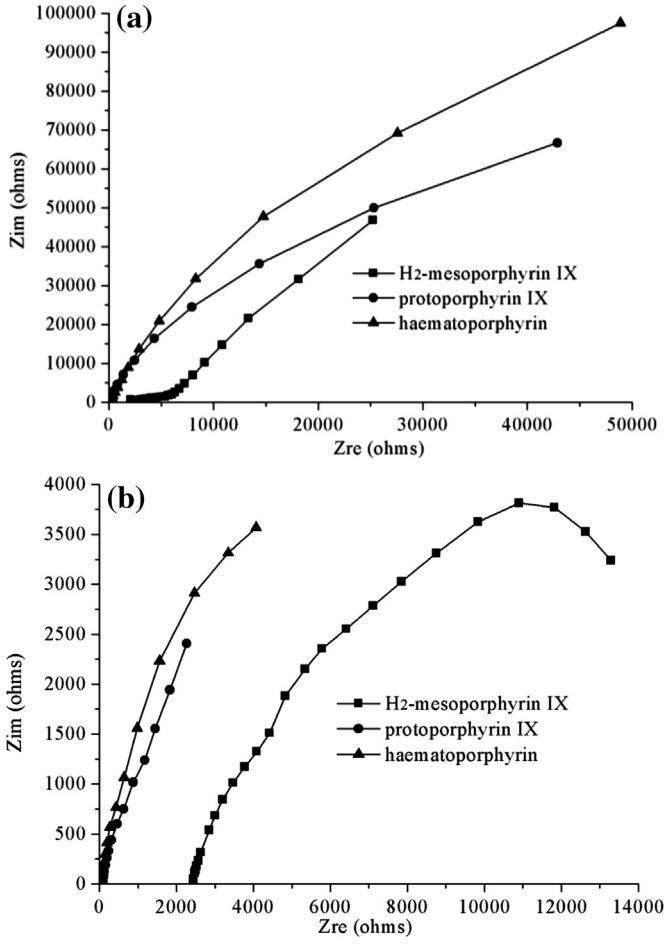

Fig. 10. The Nyquist plots of the PEBFCs fabricated with haematoporphyrin, protoporphyrin IX or H_2-mesoporphyrin IX sensitizer at the open-circuit potential (a) and 263 μA cm^{-2} (b).

3.4. EIS

EIS is a useful technique to investigate the kinetic of electron transport and recombination. To further study the effect of the sensitizer on the performance of the PEBFC, EIS was investigated in order to analyze the value of ohmic and charge transfer resistance with three sensitizers adsorbed at a mesoporous TiO_2 film electrode. The Nyquist plots for the PEBFCs were shown in Fig. 10. It demonstrated that the low-frequency arc in EIS (in the mHz range) corresponded to the Nernst diffusion within the electrolyte, the high-frequency arc (in the kHz range) reflected the charge transfer at the platinum counter electrode, and the middle-frequency arc (in the 10–100 Hz range) corresponded to the properties of the photoinjected electrons within the TiO_2. As shown in Fig. 10, for the three PEBFCs a large arc was observed, suggesting that a high resistance existed. The Nyquist plots obviously indicated that the resistance of the PEBFC decreased in the order of haematoporphyrin > protoporphyrin IX > H_2-mesoporphyrin IX. The higher charge transfer resistance is, the lower P_{max} is, therefore, the P_{max} of the PEBFC decreased in the order of H_2-mesoporphyrin IX > protoporphyrin IX > haematoporphyrin as shown in Table 4.

4. Conclusions

In summary, series of porphyrins functionalized at β-positions have been successfully used as sensitizers of photoanodes for PEBFCs to reveal the sensitizer structure–cell function relationship. The theoretical calculation showed the radiative lifetime decreased in the order of haematoporphyrin > protoporphyrin IX > H_2-mesoporphyrin IX, which was consistent with the experimental characteristic from the photocurrent action spectra measurement. The theoretical and experimental results showed that there was a close relationship among the radiative lifetime, frontier orbital energy of the porphyrins functionalized at β-positions and the photovoltaic performance of the PEBFC. The present study demonstrates that the porphyrins can be served as efficient sensitizers for the PEBFC and their performance can be enhanced by appropriate functionalization of β-positions.

Acknowledgements

This work was supported by the National Basic Research Program of China (973 Program 2011CB935702).

References

[1] B. O'Regan, M. Grätzel, Nature 353 (1991) 737–740.
[2] L.J. Luo, W. Tao, X.Y. Hu, T. Xiao, B.J. Heng, W. Huang, H. Wang, H.W. Han, Q. Jiang, J.B. Wang, Y.W. Tang, J. Power Sources 196 (2011) 10518–10525.
[3] J. Kim, H. Choi, C. Nahm, J. Moon, C. Kim, S. Nam, D.R. Jung, B. Park, J. Power Sources 196 (2011) 10526–10531.
[4] G. Veerappan, W. Kwon, S.W. Rhee, J. Power Sources 196 (2011) 10798–10805.
[5] A.T. Yahiro, S.M. Lee, D.O. Kimble, Biochim. Biophys. Acta 88 (1964) 375–383.
[6] C.F. Thurston, H.P. Bennetto, G.M. Delaney, J. Gen. Microbiol. 131 (1985) 1393–1401.
[7] G.T.R. Palmore, H. Bertschy, S.H. Bergens, G.M. Whitesides, J. Electroanal. Chem. 443 (1998) 155–161.
[8] E. Katz, I. Willner, A.B. Kotlyar, J. Electroanal. Chem. 479 (1999) 64–68.
[9] X.H. Liu, M.Q. Hao, M.N. Feng, L. Zhang, Y. Zhao, X.W. Du, G.Y. Wang, Appl. Energy 106 (2013) 176–183.
[10] L.D.L. Garza, G. Jeong, P.A. Liddell, T. Sotomura, T.A. Moore, A.L. Moore, D. Gust, J. Phys. Chem. B 107 (2003) 10252–10260.
[11] A. Brune, G. Jeong, P.A. Liddell, T. Sotomura, T.A. Moore, A.L. Moore, D. Gust, Langmuir 20 (2004) 8366–8371.
[12] M. Hambourger, A. Brune, D. Gust, A.L. Moore, T.A. Moore, Photochem. Photobiol. 81 (2005) 1015–1020.
[13] M. Hambourger, P.A. Liddell, D. Gust, A.L. Moore, T.A. Moore, Photochem. Photobiol. Sci. 6 (2007) 431–437.
[14] M. Hambourger, M. Gervaldo, D. Svedruzic, P.W. King, D. Gust, M. Ghirardi, A.L. Moore, T.A. Moore, J. Am. Chem. Soc. 130 (2008) 2015–2022.
[15] M. Hambourger, G. Kodis, M.D. Vaughn, G.F. Moore, D. Gust, A.L. Moore, T.A. Moore, Dalton Trans. (2009) 9979–9989.
[16] A. Yutaka, T. Yumi, Int. J. Hydrogen Energy 33 (2008) 2845–2849.
[17] A. Yutaka, T. Yumi, Int. J. Glob. Energy 28 (2007) 295–303.
[18] K.Q. Wang, J. Yang, L.G. Feng, Y.W. Zhang, L. Liang, W. Xing, C.P. Liu, Biosens. Bioelectron. 32 (2012) 177–182.
[19] J. Yang, L.G. Feng, F.Z. Si, Y.W. Zhang, C.P. Liu, W. Xing, K.Q. Wang, J. Power Sources 222 (2013) 344–350.
[20] M.J. Frisch, G.W. Trucks, H.B. Schlegel, G.E. Scuseria, M.A. Robb, J.R. Cheeseman, G. Scalmani, V. Barone, B. Mennucci, G.A. Petersson, H. Nakatsuji, M. Caricato, X. Li, H.P. Hratchian, A.F. Izmaylov, J. Bloino, G. Zheng, J.L. Sonnenberg, M. Hada, M. Ehara, K. Toyota, R. Fukuda, J. Hasegawa, M. Ishida, T. Nakajima, Y. Honda, O. Kitao, H. Nakai, T. Vreven, J.A. Montgomery, J.J.E. Peralta, F. Ogliaro, M. Bearpark, J.J. Heyd, E. Brothers, K.N. Kudin, V.N. Staroverov, R. Kobayashi, J. Normand, K. Raghavachari, A. Rendell, J.C. Burant, S.S. Iyengar, J. Tomasi, M. Cossi, N. Rega, J.M. Millam, M. Klene, J.E. Knox, J.B. Cross, V. Bakken, C. Adamo, J. Jaramillo, R. Gomperts, R.E. Stratmann, O. Yazyev, A.J. Austin, R. Cammi, C. Pomelli, J.W. Ochterski, R.L. Martin, K. Morokuma, V.G. Zakrzewski, G.A. Voth, P. Salvador, J.J. Dannenberg, S. Dapprich, A.D. Daniels, O. Farkas, J.B. Foresman, J.V. Ortiz, J. Cioslowski, D.J. Fox, Gaussian 09. Revision A. 01, Gaussian Inc, Wallingford CT, 2009.
[21] A.D. Becke, J. Chem. Phys. 98 (1993) 5648–5652.
[22] C. Lee, W. Yang, R.G. Parr, Phys. Rev. B 37 (1988) 785–789.
[23] A.S. Hart, K.C. Chandra Bikram, N.K. Subbaiyan, P.A. Karr, F. D'Souza, Appl. Mater. Interfaces 4 (2012) 5813–5820.
[24] Y.M. Cao, Y. Bai, Q.J. Yu, Y.M. Cheng, S. Liu, D. Shi, F.F. Gao, P. Wang, J. Phys. Chem. C 113 (2009) 6290–6297.
[25] A. Hagfeldf, M. Grätzel, Chem. Rev. 95 (1995) 49–68.
[26] J.A. Mikroyannidis, G. Charalambidis, A.G. Coutsolelosb, P. Balraju, G.D. Sharma, J. Power Sources 196 (2011) 6622–6628.
[27] M.J. Lee, K.D. Seo, H.M. Song, M.S. Kang, Y.K. Eom, H.S. Kang, H.K. Kim, Tetrahedron Lett. 52 (2011) 3879–3882.
[28] N. Xiang, W.P. Zhou, S.H. Jiang, L.J. Deng, Y.J. Liu, Z. Tan, B. Zhao, P. Shen, S.T. Tan, Sol. Energy Mater. Sol. Cells 95 (2011) 1174–1181.
[29] Y. Tachibana, S.A. Haque, I.P. Mercer, J.R. Durrant, D.R. Klug, J. Phys. Chem. B 104 (2000) 1198–1205.
[30] A. Kay, M. Grätzel, J. Phys. Chem. 97 (1993) 6272–6277.
[31] T.L. Ma, K. Inoue, K. Yao, H. Noma, T. Shuji, E. Abe, J.H. Yu, X.S. Wang, B.W. Zhang, J. Electroanal. Chem. 537 (2002) 31–38.
[32] D. Shi, Y.M. Cao, N. Pootrakulchote, Z.H. Yi, M.F. Xu, S.M. Zakeeruddin, M. Grätzel, P. Wang, J. Phys. Chem. C 112 (2008) 17478–17485.
[33] V. Shklover, Y.E. Ovchinnikov, L.S. Braginsky, S.M. Zakeeruddin, M. Grätzel, Chem. Mater. 10 (1998) 2533–2541.
[34] A.O.T. Patrocínio, E.B. Paniago, R.M. Paniago, N.Y. Murakami Iha, Appl. Surf. Sci. 254 (2008) 1874–1879.
[35] H. Spanggaard, F.C. Krebs, Sol. Energy Mater. Sol. Cells 83 (2004) 125–146.
[36] J. Yin, L. Qi, H.Y. Wang, Appl. Mater. Interfaces 3 (2011) 4315–4322.
[37] K. Takechi, T. Shiga, T. Motohiro, T. Akiyama, S. Yamada, H. Nakayama, K. Kohama, Sol. Energy Mater. Sol. Cells 90 (2006) 1322–1330.
[38] A. Kathiravan, R. Renganathan, J. Colloid Interface Sci. 331 (2009) 401–407.
[39] K.K. Wong, A. Ng, X.Y. Chen, Y.H. Ng, Y.H. Leung, K.H. Ho, A.B. Djurišić, A.M.C. Ng, W.K. Chan, L.H. Yu, D.L. Phillips, Appl. Mater. Interfaces 4 (2012) 1254–1261.